Evolution of the electronic structure in partially filled skutterudites: $Ca_xCo_4Sb_{12}$ studied using NMR

C. S. Lue* and S. C. Chen
Department of Physics, National Cheng Kung University, Tainan 70101, Taiwan
(Received 4 January 2009; revised manuscript received 13 February 2009; published 11 March 2009)

^{59}Co nuclear magnetic resonance (NMR) investigations are presented for the partially filled skutterudites $Ca_xCo_4Sb_{12}$ with $x \leq 0.2$. For low Ca concentrations ($x \leq 0.13$), the temperature-dependent isotropic Knight shifts and spin-lattice relaxation rates are accounted for by semiconducting characteristics, with a trend of the reduction in the band gap as increasing the Ca content. For a higher Ca concentration ($x=0.2$), the NMR features can be described well in terms of a semimetallic response as the corresponding Fermi level falling within a pseudogap formed by nearby bands. With these respects, the present NMR results provide a microscopic picture that a semiconducting-semimetallic transition occurs as the filling fraction $0.13 < x < 0.2$ in $Ca_xCo_4Sb_{12}$.

DOI: 10.1103/PhysRevB.79.125108 PACS number(s): 76.60.−k, 71.55.Ak, 71.20.−b

I. INTRODUCTION

Filled skutterudites with the general formula MT_4X_{12} (where M can be an alkaline earth, a lanthanide, or an actinide ion; T is a transition metal such as Fe, Co, or Ru; and X is P, As, or Sb) have attracted considerable attention due to their unusual electronic and magnetic properties. The phenomena including superconductivity, ferromagnetism, metal-semiconductor transitions, heavy fermion behavior, and non-Fermi liquid behavior exist in this class of materials.[1–7] Among these alloys, the $CoSb_3$-based skutterudites have been realized as promising candidates for the thermoelectric applications.[8] The unfilled skutterudite $CoSb_3$ crystallizes in the cubic $CoAs_3$-type structure (space group $Im\bar{3}$). As shown in Fig. 1, a large fraction of voids appears in this crystal structure, and these voids can be partially inserted by various elements such as Ca, Sr, La, and Ce, to form the $M_xCo_4Sb_{12}$ skutterudites, where x is its filling fraction.[9] These fillers have an effect to reduce the lattice thermal conductivity through the scattering of the thermal phonons by the rattling of the filled atoms.[3,10–17] It thus improves the thermoelectric performance according to the figure of merit $Z=S^2\sigma/\kappa$, where S and σ are the Seebeck coefficient and electrical conductivity and κ represents the thermal conductivity of the material. In addition to the reduction in κ as filling different atoms in the voids of $CoSb_3$, S, and σ may be enhanced in accordance with the change in electronic structures in the vicinity of the Fermi surfaces.

The electronic property of $CoSb_3$ has been classified as a narrow band-gap p-type semiconductor. It has been found that a metal-semiconductor transition accompanying a sign reversal of the Seebeck coefficient and Hall coefficient usually takes place as filling atoms in the voids of $CoSb_3$.[18] Many efforts have been made to realize the evolution of the band structures in $M_xCo_4Sb_{12}$, especially focusing on the interpretation of the measured transport properties and the prediction of the optimum thermoelectric performance.[19–23] To provide a microscopic insight on the evolution of the electronic structure via filling atoms in the voids, we study the $Ca_xCo_4Sb_{12}$ system using the nuclear magnetic resonance (NMR) technique which is known as an atomic probe in paramagnetic alloys yielding information about the Fermi surface features.[24] Since the insertion of the divalent Ca ions is expected to have a relative moderate effect on the change in the electronic properties as compared to the filling with trivalent ions such as Y^{3+} and La^{3+}, a progressive transition from a semiconducting state to a (semi)metallic state could be possibly observed for the case of $Ca_xCo_4Sb_{12}$.

In this investigation, ^{59}Co NMR results including the powder pattern, the Knight shift, and the spin-lattice relaxation rate of $Ca_xCo_4Sb_{12}$ with $x=0.05$, 0.13, and 0.2 are presented. To provide a clear trend for the variation in electronic features from unfilled to partially Ca filled skutterudites, we include the previously reported data of $CoSb_3$. The NMR observations indicate the semiconducting characteristics for $Ca_{0.05}Co_4Sb_{12}$ and $Ca_{0.13}Co_4Sb_{12}$ while $Ca_{0.2}Co_4Sb_{12}$ behaves as a semimetal. These results are in good agreement with the observations from other experiments as well as those from band-structure calculations.

II. EXPERIMENTAL DETAILS

Polycrystalline $Ca_xCo_4Sb_{12}$ compounds were prepared from 99.9% Ca, 99.95% Co, and 99.999% Sb by mixing

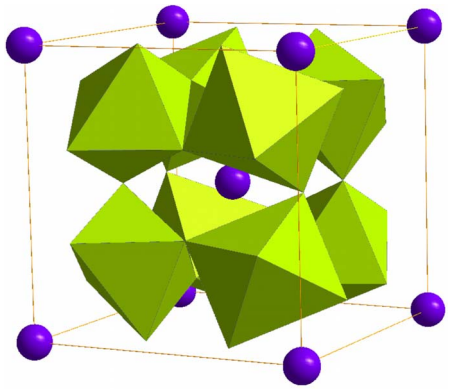

FIG. 1. (Color online) The filled skutterudite structure of MCo_4Sb_{12}. Each of the octahedra is $CoSb_6$ in which the Co atom is located at the center and the Sb atoms occupy the corners. The large spheres represent the voids which can be partially filled by various M atoms.

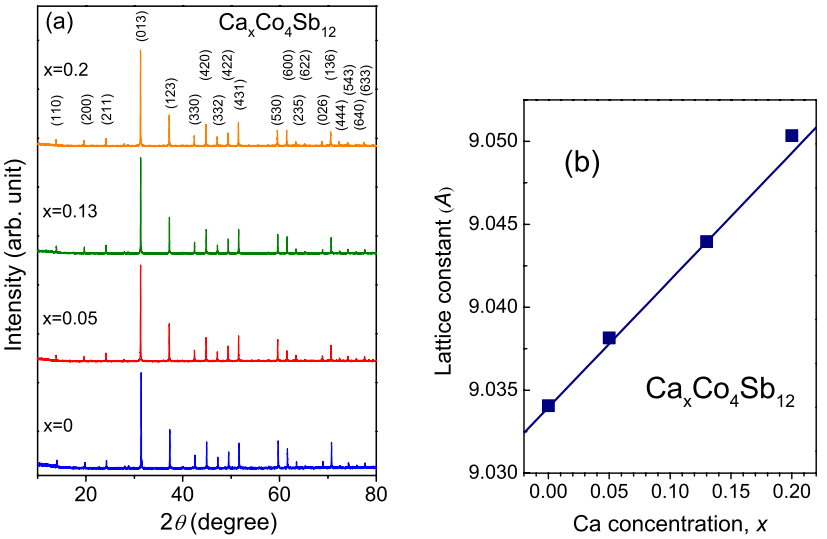

FIG. 2. (Color online) (a) X-ray diffraction patterns for $Ca_xCo_4Sb_{12}$ with $x=0$, 0.05, 0.13, and 0.2. (b) Lattice constant as a function of the Ca concentration x. The corresponding straight line is guide for the eyes for the linear tendency.

appropriate amounts of elemental metals and were melted in an induction furnace under partial argon atmosphere. Due to the volatility of Sb at high temperatures, we started with an excess of 3 mol % from stoichiometry for Sb. To promote homogeneity, the resulting ingots were annealed in a vacuum-sealed quartz tube at 800 °C for 3 days followed by furnace cooling. For each specimen, an x-ray analysis taken with Cu $K\alpha$ radiation shows a single phase, as demonstrated in Fig. 2(a). All reflection peaks in the corresponding diffraction spectrum could be indexed according to the expected $CoAs_3$-type structure.

The variation in the lattice constant as a function of the Ca concentration is plotted in Fig. 2(b). It is clear that the lattice constant increases with the Ca filling level, indicating that the voids of $CoSb_3$ are successfully filled by Ca, according to Vegard's law. This is also consistent with the result of synthesis using a solid-state reaction growth method.[25] As a matter of fact, the highest filling fraction of $x=0.2$ in this study is within the solubility limit of $x_c \simeq 0.22$ for Ca in the voids of $CoSb_3$ predicted by a theoretical calculation.[26,27]

NMR experiments were performed using a Varian 300 spectrometer, with a homebuilt probe employed for both room-temperature and low-temperature measurements. Each powdered specimen was put in a plastic vial that showed no observable ^{59}Co NMR signal. The Knight shift here was referred to the ^{59}Co resonance frequency of one molar aqueous $K_3Co(CN)_6$.

A. Powder pattern

Within the ordered cubic $Im\bar{3}$ structure, the axially symmetric Co site results in a one-site NMR spectrum for each of the studied composition. Because of the electric quadrupole coupling, the ^{59}Co NMR spectrum ($I=\frac{7}{2}$) consists of a main line (shown in Fig. 4) flanked by six satellite lines, as illustrated in Fig. 3. For the powder specimens, as in our experiment, these lines exhibit as a typical powder pattern, with the distinctive edges corresponding to the quadrupole parameter. Since the first-order quadrupole interaction is the main effect shaping these lines, the quadrupole frequency, ν_Q, was estimated directly from these lines. The determined ν_Q values were summarized in Table I. It is clear that ν_Q gradually decreases with increasing x in $Ca_xCo_4Sb_{12}$, pointing to a reduction in the local electric-field gradient (EFG) via Ca filling.

It is apparent that the sharpness of the satellite line edge gradually smears out with increasing the Ca filling content in the voids of $CoSb_3$, and this feature is mainly due to the randomness of the local EFG that is known to broaden the satellite line effectively. Note that this is a static effect due to the randomness occupation of the voids by Ca atoms. In addition, one may speculate that the observed line broadening could be related to the rattling of Ca, which is expected to reduce with decreasing temperature. The NMR linewidths for all studied compositions are, however, almost temperature independent, indicating that the rattling has negligible effect on the line broadening.

Room-temperature central transition ($m=\frac{1}{2}\leftrightarrow-\frac{1}{2}$) line shapes for $Ca_xCo_4Sb_{12}$ are displayed in Fig. 4. The observed

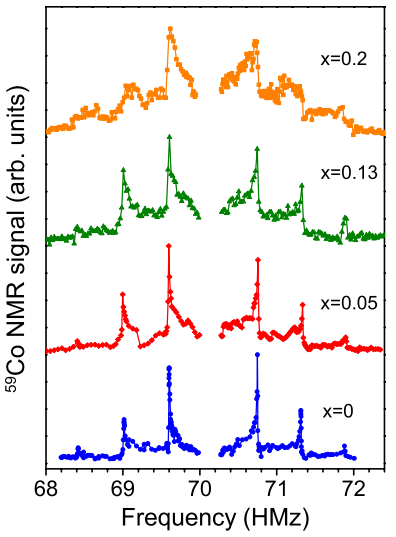

FIG. 3. (Color online) Resolved ^{59}Co NMR satellite lines for $Ca_xCo_4Sb_{12}$.

TABLE I. Quadrupole frequency, axial Knight shift, T-independent isotropic Knight shift, prefactor A in units 10^{-5} s^{-1} K^{-2}, gap size, and inverse Korringa constant in units s^{-1} K^{-1} of $Ca_xCo_4Sb_{12}$.

x	ν_Q (MHz)	K_{ax} (%)	K_o (%)	A	Δ (K)	$1/T_{1K}T$
0	1.180	−0.039	−0.043	1.4	460	0
0.05	1.165	−0.038	−0.048	8.9	170	0
0.13	1.145	−0.040	−0.049	14	130	0
0.20	1.125	−0.037	−0.075	71	80	0.079

spectrum splits into two peaks because of the presence of the second-order quadrupole interactions. Similar to the satellite lines, the central transition linewidth gradually broadens with adding the Ca content. This could be also ascribed to an increase in the degree of the EFG inhomogeneity. It is important to mention that the feature of the line shapes remains unchanged with temperature, indicative of the nonmagnetic nature for $Ca_xCo_4Sb_{12}$. This characteristic confirms that the filling of Ca in the voids of $CoSb_3$ does not induce noticeable magnetic moments on the Co sites.

We performed a central line-shape simulation with a proper broadening factor to reproduce the synthetic spectrum for each individual composition. For a polycrystalline sample, the shape function simulation for the combination of the quadrupole and the anisotropic Knight shift interactions was first presented by Jones *et al.*[28] Due to the cubic structure of $Ca_xCo_4Sb_{12}$, the ^{59}Co quadrupole shift and the angle-dependent Knight shift are axially symmetric. Therefore, the frequency of the central transition is given by

$$\nu = \nu_o\left[1 + \frac{K_{ax}}{1+K_{iso}}(3\cos^2\theta - 1) + \frac{15}{16}\left(\frac{\nu_Q}{\nu_o}\right)^2(1-\cos^2\theta)(1-9\cos^2\theta)\right], \quad (1)$$

where ν_o is the Larmor frequency, K_{iso} is the isotropic Knight shift, K_{ax} is the axial Knight shift, and θ is the angle between the crystal symmetry axis and the external magnetic field. To compute the line shape appropriate to a polycrystalline sample, the line-shape function is, following Cohen and Reif,[29]

$$P(\nu-\nu_o) = \frac{1}{2}\left|\frac{d\nu}{d\cos\theta}\right|^{-1}. \quad (2)$$

According to Eq. (1), the shape function possesses a step at $\nu_S = \nu_o + 2a\nu_o$ and two singularities at the high frequency $\nu_H = \nu_o + b/\nu_o - a\nu_o$ and the low frequency $\nu_L = \nu_o - 16b/9\nu_o - 2a\nu_o/3 - 2a^2\nu_o^3/4b$, where $a = K_{ax}/1+K_{iso}$ and $b = 15\nu_Q^2/16$ for $I = 7/2$. By substituting b and tuning a, the synthetic profile was thus obtained and can match well with the experimental ^{59}Co NMR spectra. For each material, the best-simulated result is shown as a dotted curve in Fig. 4. The simulations yield the corresponding K_{iso} (indicated by an arrow) and K_{ax} values (listed in Table I).

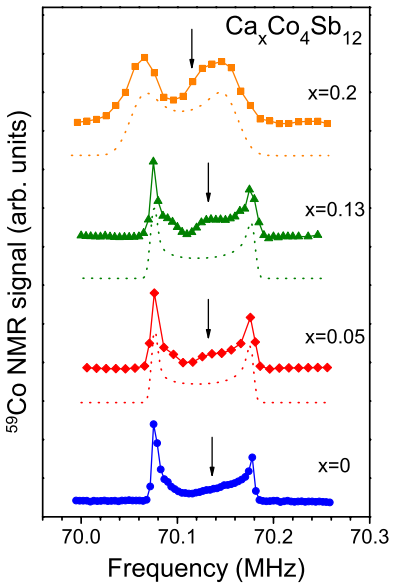

FIG. 4. (Color online) Room-temperature ^{59}Co NMR central transition spectra for $Ca_xCo_4Sb_{12}$. The simulated results, drawn as dotted curves, have been shifted down for clarity. Each arrow indicates the frequency for the isotropic Knight shift.

B. Knight shift

Figure 5 shows the temperature dependence of ^{59}Co NMR isotropic Knight shifts for $Ca_xCo_4Sb_{12}$. The observation can be simply separated by two terms: $K_{iso}(T) = K_o + K(T)$. The first term K_o is T independent and can be estimated from the low-temperature limit. The determined K_o values were tabulated in Table I. Since the sign of K_o is negative and the magnitudes for $CoSb_3$, $Ca_{0.05}Co_4Sb_{12}$, and $Ca_{0.13}Co_4Sb_{12}$ are quite tiny, these terms can be attributed to the diamagnetic shift, commonly observed in insulating materials.[30] For $Ca_{0.2}Co_4Sb_{12}$, however, the K_{iso} data lie well below the others, corresponding to a relative large absolute value of K_o. We associated this observation with the additional contribution from the d-spin shift (K_d) since K_d is negative due to the negative d-electron hyperfine coupling for the core-polarization mechanism.[31] In paramagnetic metals and semimetals, K_d is usually proportional to the partial d-electron Fermi-level density of states (DOS), $N_d(E_F)$. It thus indicates nonzero Co $3d$ states at the Fermi level, implying the disap-

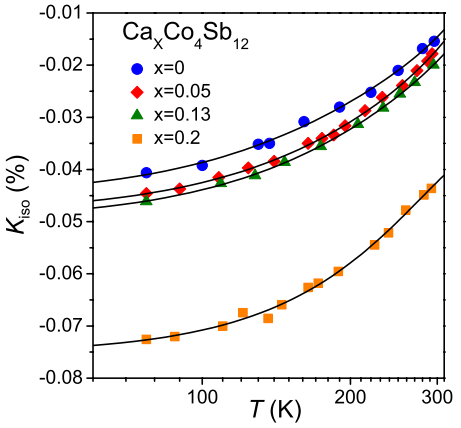

FIG. 5. (Color online) Temperature dependence of the ^{59}Co isotropic Knight shift for $Ca_xCo_4Sb_{12}$. The solid curves are guide for the eyes for clarity.

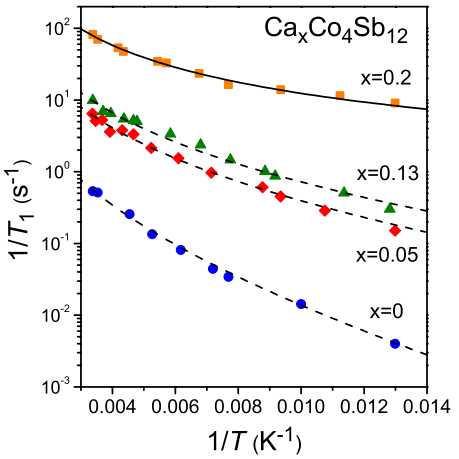

FIG. 6. (Color online) Temperature variation of ^{59}Co the spin-lattice relaxation rate for $Ca_xCo_4Sb_{12}$. Dashed curves: fit to the semiconducting behavior for $CoSb_3$, $Ca_{0.05}Co_4Sb_{12}$, and $Ca_{0.13}Co_4Sb_{12}$. Solid curve: fit to the semimetallic character from Eq. (3) for $Ca_{0.2}Co_4Sb_{12}$.

pearance of the band gap in $Ca_{0.2}Co_4Sb_{12}$. In fact, this is consistent with the low-temperature specific-heat measurement on $Ca_{0.2}Co_4Sb_{12}$ which showed a relative high electronic specific-heat coefficient $\gamma=28$ mJ/mol K^2, confirming the existence of a finite DOS at E_F.[18]

On the other hand, the T-dependent part $K(T)$ reflects an increase in the spin susceptibility, attributed to a thermally activated increase in the number of carriers, also responsible for the enhancement in the relaxation rate. Note that the shift to higher frequencies with increasing temperature cannot be associated with the negative core polarization induced by the spin susceptibility of cobalt d states. Contrary to other gapped systems such as Fe_2VAl and Fe_2VGa,[32,33] the ^{51}V Knight shifts were found to shift to lower frequencies with increasing temperature, attributed to the negative core polarization of vanadium d states. With this respect, we conclude that the thermally excited carriers in $Ca_xCo_4Sb_{12}$ are mainly s character, with positive s-hyperfine constant responsible for the T-dependent Knight shifts and spin-lattice relaxation rates at elevated temperatures.

C. Spin-lattice relaxation rate

Temperature dependence of the spin-lattice relaxation rate $(1/T_1)$ was measured using the saturation recovery method. The saturation rf comb with 50 short 2 μs pulses was employed. We recorded the recovery of the signal strength by integrating the ^{59}Co spin echo signal. In this experiment, the relaxation process involves transitions between adjacent spin levels $\Delta m=\pm 1$ that have different probabilities because of the quadrupole splitting. Therefore, the corresponding spin-lattice relaxation obeys a multiexponential expression. T_1 values were thus obtained by fitting to a multiexponential recovery curve for $I=7/2$. In Fig. 6, we show a plot of $1/T_1$ versus inverted temperature for the studied $Ca_xCo_4Sb_{12}$ alloys. For comparison, we include the previous result of $CoSb_3$ in the figure.[30] It is apparent that the temperature variation of $1/T_1$ for $Ca_{0.05}Co_4Sb_{12}$ and $Ca_{0.13}Co_4Sb_{12}$ is quite similar to that of $CoSb_3$, exhibiting thermally activated behavior within the measured temperature range. On the other hand, the T-dependent $1/T_1$ for $Ca_{0.2}Co_4Sb_{12}$ shows a semimetallic characteristic with a metallic feature at low temperatures and an activated response upon rising temperature.

With these respects, the $1/T_1T$'s of $Ca_xCo_4Sb_{12}$ can be expressed as[34]

$$\frac{1}{T_1T}=\frac{1}{T_{1K}T}+ATe^{-\Delta/2k_BT}. \quad (3)$$

The first term $1/T_{1K}T$ is the inverse Korringa constant which is generally associated with the partial Fermi-level DOS of the probed site and should be zero for the presence of a band gap at the Fermi level. The second part is due to the band edge separated from the Fermi level. This form assumes an effective-mass approximation for the band edge, with the prefactor A associated with the effective mass of carriers as well as their concentrations. Each carrier density varies with temperature according to $T^{3/2}\exp(-\Delta/2k_BT)$. For $CoSb_3$, $Ca_{0.05}Co_4Sb_{12}$, and $Ca_{0.13}Co_4Sb_{12}$, the observed $1/T_1T$ data can be fitted well to Eq. (3) with $1/T_{1K}T=0$, shown as dashed curves in Fig. 6. However, the $1/T_1T$ data of $Ca_{0.2}Co_4Sb_{12}$ cannot be reproduced according to Eq. (3) with the fixed $1/T_{1K}T=0$. Instead, a fit to Eq. (3) using $1/T_{1K}T$, A, and Δ as parameters was performed for this composition. It is remarkable that this fits quite well over the entire temperature range, with the fitting result plotted as a solid curve passing through the experimental data points. From these analyses, the values of $1/T_{1K}T$, A, and Δ were thus extracted with the results summarized in Table I. It should be noted that the values of $1/T_1$ in $Ca_{0.2}Co_4Sb_{12}$ are about ten times larger than those in $Ca_{0.05}Co_4Sb_{12}$ and $Ca_{0.13}Co_4Sb_{12}$ (more than 2 orders of magnitude greater than $CoSb_3$), implying that the number of the s-character carriers is substantially enhanced as filling a higher Ca concentration in the voids of $CoSb_3$.

III. DISCUSSION

We have classified $CoSb_3$, $Ca_{0.05}Co_4Sb_{12}$, and $Ca_{0.13}Co_4Sb_{12}$ as narrow band-gap semiconductors while $Ca_{0.2}Co_4Sb_{12}$ is a semimetal through NMR observations. The gap gradually reduces with filling Ca but remains open at least up to $x=0.13$ in $Ca_xCo_4Sb_{12}$. Since the *s*-character carriers are responsible for the activated response, the decrease in the gap size can be easily understood as the broadening of the *s* states. This interpretation is in good agreement with the increasing trend of the prefactor A of the thermally activated nuclear relaxation in $Ca_xCo_4Sb_{12}$ as the constant A is essentially associated with the effective mass of the carriers and their concentrations. Indeed, Puyet *et al.*[18] reported an increase in the number of carriers with the Ca content of $Ca_xCo_4Sb_{12}$ being consistent with our NMR results. With further addition of Ca, the gap tends to close, resulting in a pseudogap in the vicinity of the Fermi level as for the case of $x=0.2$. The nonsemiconducting nature has been confirmed by the existence of a relative large γ in $Ca_{0.2}Co_4Sb_{12}$, revealed from the low-temperature specific-heat measurement.[18]

According to a recent theoretical calculation on $Ca_xCo_4Sb_{12}$, the Co 3*d* bands are all at the Fermi level with very few *s*-character electrons near the Fermi surface.[18] On this basis, the Korringa relaxation process for $Ca_{0.2}Co_4Sb_{12}$ is dominated by the *d*-spin relaxation rate and can be expressed as

$$\frac{1}{T_{1K}T} = 2hk_B[\gamma_n H_{\mathrm{hf}}^d N_d(E_F)]^2 q. \quad (4)$$

Here h, k_B, and γ_n are the Planck constant, the Boltzmann constant, and the ^{59}Co nuclear gyromagnetic ratio, respectively. $N_d(E_F)$ is the Co 3*d* Fermi-level DOS in units of states/eV spin. H_{hf}^d represents the core-polarization hyperfine field per electron, taken to be -1.8×10^5 G for cobalt-based metals,[35] and q is a reduction factor equal to the reciprocal of the degeneracy. For electron pockets located at Γ, as revealed from band-structure calculations,[18] the cobalt *d*-electron manifold has three degeneracies, giving $q=1/3$. With these parameters and experimental $1/T_{1K}T=0.079$ s^{-1} K^{-1}, we obtain $N_d(E_F)=0.51$ states/eV spin for $Ca_{0.2}Co_4Sb_{12}$. Interestingly, this value is close to the calculated $N_d(E_F)=0.58$ states/eV spin (deduced from Fig. 10 in Ref. 18), supporting the reliable $1/T_{1K}T$ analysis presented here.

It is worthwhile comparing the present NMR results of $Ca_xCo_4Sb_{12}$ with those of the La-filled skutterudites. In fact, the insertion of La in the voids of $CoSb_3$ has been found to affect more markedly on the electronic features where a significant decrease in ν_Q, a rapid increase in $|K_o|$, and a strong enhancement in the Fermi-level DOS have been found.[36] It thus results in the quick disappearance of the semiconducting characteristics with a small La content such as $La_{0.1}Co_4Sb_{12}$. Since the addition of the fillers effectively behaves as doping electrons in $CoSb_3$, the different response between these two systems can be simply associated with the different charge valence of the filled ions. As the La^{3+} ion is trivalent while Ca^{2+} is divalent, the Ca filling should have a weaker effect on the band-structure modification. As a consequence, a progressive transition from a semiconducting state to a semimetallic state can be observed in $Ca_xCo_4Sb_{12}$.

IV. CONCLUSIONS

NMR measurements have provided a local picture of the electronic properties in $Ca_xCo_4Sb_{12}$. For $x\leq0.13$, the observed isotropic Knight shifts and spin-lattice relaxation rates are understood in terms of the semiconducting behavior, with a trend of the reduction in the band gap as increasing the Ca content. For a higher Ca concentration ($x=0.2$), the NMR features can be associated with a semimetallic response as the corresponding Fermi level located within a pseudogap formed by nearby bands.

ACKNOWLEDGMENTS

We are grateful to M. W. Chu of the Center for Condensed Matter Sciences in National Taiwan University for the help with x-ray measurements. This work was supported by the National Science Council of Taiwan under Grant No. NSC-95-2112-M-006-021-MY3 (C.S.L).

*cslue@mail.ncku.edu.tw

[1] G. P. Meisner, Physica B & C **108B**, 763 (1981).
[2] M. S. Torikachvili, M. B. Maple, and G. P. Meisner, in *Proceedings of LT-17*, edited by U. Ekern, A. Shmid, W. Weber, and W. Wuhl (Elsevier, Amsterdam, 1984), p. 711.
[3] B. C. Sales, D. Mandrus, and R. K. Williams, Science **272**, 1325 (1996).
[4] C. Sekine, T. Uchiumi, I. Shirotani, and T. Yagi, Phys. Rev. Lett. **79**, 3218 (1997).
[5] N. A. Frederick, T. D. Do, P.-C. Ho, N. P. Butch, V. S. Zapf, and M. B. Maple, Phys. Rev. B **69**, 024523 (2004).
[6] M. B. Maple, N. A. Frederick, P.-C. Ho, W. M. Yuhasz, and T. Yanagisawa, J. Supercond. Novel Magn. **19**, 299 (2007), and references therein.
[7] S. Masaki, T. Mito, S. Wada, H. Sugawara, D. Kikuchi, and H. Sato, Phys. Rev. B **78**, 094414 (2008).
[8] C. Uher, Semicond. Semimetals **69**, 139 (2001), and references therein.
[9] G. S. Nolas, D. T. Morelli, and T. M. Tritt, Annu. Rev. Mater. Sci. **29**, 89 (1999), and references therein.
[10] G. A. Slack and V. G. Tsoukala, J. Appl. Phys. **76**, 1665 (1994).
[11] D. T. Morelli and G. P. Meisner, J. Appl. Phys. **77**, 3777 (1995).
[12] G. S. Nolas, G. A. Slack, D. T. Morelli, T. M. Tritt, and A. C. Ehrlich, J. Appl. Phys. **79**, 4002 (1996).
[13] B. Chen, J. H. Xu, C. Uher, D. T. Morelli, G. P. Meisner, J. P. Fleurial, T. Caillat, and A. Borshchevsky, Phys. Rev. B **55**, 1476 (1997).
[14] D. T. Morelli, G. P. Meisner, B. Chen, S. Hu, and C. Uher, Phys.

Rev. B **56**, 7376 (1997).
[15] G. S. Nolas, M. Kaeser, R. T. Littleton IV, and T. M. Tritt, Appl. Phys. Lett. **77**, 1855 (2000).
[16] J. Yang, D. T. Morelli, G. P. Meisner, W. Chen, J. S. Dyck, and C. Uher, Phys. Rev. B **67**, 165207 (2003).
[17] V. L. Kuznetsov, L. A. Kuznetsova, and D. M. Rowe, J. Phys.: Condens. Matter **15**, 5035 (2003).
[18] M. Puyet, B. Lenoir, A. Dauscher, P. Pecheur, C. Bellouard, J. Tobola, and J. Hejtmanek, Phys. Rev. B **73**, 035126 (2006).
[19] D. J. Singh and I. I. Mazin, Phys. Rev. B **56**, R1650 (1997).
[20] G. P. Meisner, D. T. Morelli, S. Hu, J. Yang, and C. Uher, Phys. Rev. Lett. **80**, 3551 (1998).
[21] L. Bertini and C. Gatti, J. Chem. Phys. **121**, 8983 (2004).
[22] L. Chaput, P. Pecheur, J. Tobola, and H. Scherrer, Phys. Rev. B **72**, 085126 (2005).
[23] K. Mangersnes, O. M. Lovvik, and O. Prytz, New J. Phys. **10**, 053004 (2008).
[24] C. S. Lue, T. H. Su, B. X. Xie, and C. Cheng, Phys. Rev. B **74**, 094101 (2006).
[25] M. Puyet, B. Lenoir, A. Dauscher, P. Weisbecker, and S. J. Clarke, J. Solid State Chem. **177**, 2138 (2004).
[26] X. Shi, W. Zhang, L. D. Chen, and J. Yang, Phys. Rev. Lett. **95**, 185503 (2005).
[27] X. Shi, W. Zhang, L. D. Chen, J. Yang, and C. Uher, Phys. Rev. B **75**, 235208 (2007).
[28] W. H. Jones, Jr., T. P. Graham, and R. G. Barnes, Phys. Rev. **132**, 1898 (1963).
[29] M. H. Cohen and F. Reif, in *Solid State Physics*, edited by F. Seitz and D. Turnbull (Academic, New York, 1957), Vol. 5, p. 311.
[30] C. S. Lue, Y. T. Lin, and C. N. Kuo, Phys. Rev. B **75**, 075113 (2007).
[31] *Metallic Shifts in NMR*, edited by G. C. Carter, L. H. Bennett, and D. J. Kahan (Pergamon, Oxford, 1977).
[32] C.-S. Lue and Joseph H. Ross, Jr., Phys. Rev. B **58**, 9763 (1998).
[33] C. S. Lue and Joseph H. Ross, Jr., Phys. Rev. B **63**, 054420 (2001).
[34] N. Bloembergen, Physica **20**, 1130 (1954); Dieter Wolf, *Spin Temperature and Nuclear-spin Relaxation in Matter* (Clarendon, Oxford, 1979).
[35] K. Yoshimura, M. Mekata, M. Takigawa, Y. Takahashi, and H. Yasuoka, Phys. Rev. B **37**, 3593 (1988).
[36] C. S. Lue, S. M. Huang, C. N. Kuo, F.-T. Huang, and M.-W. Chu, New J. Phys. **10**, 083029 (2008).